Volume 1 | Number 1 | Jan 2013 | Pages 1–100

Journal of
Materials Chemistry A

Materials for energy and sustainability
www.rsc.org/materialsA

Li⁺

ROYAL SOCIETY
OF CHEMISTRY

ROYAL SOCIETY
OF CHEMISTRY

www.rsc.org/materialsA

Journal of Materials Chemistry A

Increased Activity in Hydrogen Evolution Electrocatalysis for Partial Anionic Substitution in Cobalt Oxysulfide Nanoparticles[†]

Andrew Nelson,[a §] Kevin E. Fritz,[a §] Shreyas Honrao,[a b] Richard G. Hennig,[b a] Richard D. Robinson,[a ‡] and Jin Suntivich[a c ‡]

The functionality of an electrocatalyst depends sensitively on the surface chemistry. In the case of transition-metal compounds, both the transition metal cation and the anion must be controlled to maximize the electrocatalytic activity. This realization has driven many efforts devoted to engineering the cation chemistry, producing many state-of-the-art electrocatalysts. Motivated by the critical role the cation plays in electrocatalysis, we seek to understand whether a similar effect can be achieved with the anion. Herein, we present a study on the effect of the anion substitution on the hydrogen evolution reaction (HER) electrocatalysis on cobalt oxysulfide nanoparticles. To control the sulfur substitution, we use ammonium sulfide to introduce sulfur to the cobalt oxide nanoparticles at low temperature without inducing secondary phase formation. We find that a lightly doped oxysulfide catalyst, which has the composition $CoO_xS_{0.18}$, exhibits a metastable, distorted S-substituted CoO phase and is 2-3 times more active for the HER than either end-member of the substitution series. Our first-principles calculations attribute the HER enhancement to the stronger surface H adsorption which is maximally favorable at a relatively low doping level. Our work provides a protocol for synthesizing metastable mixed-anion materials and reveals the critical role of the anion on the surface physiochemical properties and the HER electrocatalysis.

One of the largest factors limiting the commercialization of air-breathing electrochemical energy storage technologies lies in the requirement of rare, precious-metal catalysts.[1-10] Transition-metal-containing compounds such as oxides,[10-15] chalcogenides,[16-21] and pnictides[22-24] exhibit high activities and are attractive alternatives to rare, precious metals. The pursuit of these transition-metal-containing electrocatalysts has driven many efforts[11, 25, 26] in controlling physicochemical properties

such as the surface-adsorbate interaction[27, 28] to find the most electrocatalytically active surface.[1, 2, 11] Thus far, approaches based on cationic substitutions have been highly successful in controlling the surface-adsorbate interaction for engineering the electrocatalytic activities.[25, 29, 30] These investigations have produced many mixed-cation electrocatalysts that are considered the state-of-the-art.[11, 13, 25, 29, 31, 32]

Considering these positive results from cationic substitution, a natural question is whether a similar substitution of the anion can also benefit the activity of the transition-metal-containing electrocatalysts. Transition metal compounds with mixed anions have been explored for batteries,[33] transparent conducting oxides,[34] photocatalysts,[35, 36] and electrocatalysts. In electrocatalysis, many works using mixed anionic compounds such as MoS_2-$MoSe_2$,[37] MoO_x-MoS_2,[38, 39] sulfidized MoP,[40] phosphidized CoS_2,[41] selenized Ni_2P,[42] or amorphous Co-O-S[43] have established that mixed anions can lead to superior performance. Still, it is not clear how the anion substitution affects the physicochemical and electrocatalytic properties. This is partly because many of these studies have focused
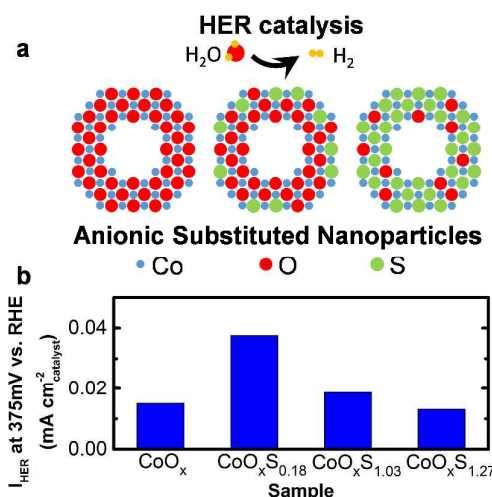

Figure 1. Schematic of the anionic substitution in CoO_x nanoparticles as a testbed for HER electrocatalysis (**a**). Results from this work indicate that the maximum HER activity occurs at low doping levels (e.g., $CoO_xS_{0.18}$), while at higher doping levels, activity decreases (**b**). The HER activity is normalized to the surface areas of the catalysts.

a. Department of Materials Science and Engineering, Cornell University, Ithaca, NY, 14853, USA
b. Department of Materials Science and Engineering, University of Florida, Gainesville, FL, 32611, USA
c. Kavli Institute at Cornell for Nanoscale Science, Cornell University, Ithaca, NY, 14853, USA
§ These authors contributed equally to this work.
‡ Corresponding authors. Email: rdr82@cornell.edu and jsuntivich@cornell.edu
†Electronic Supplementary Information (ESI) available: experimental details, further discussion of electron diffraction data, electron diffraction data for annealed samples, particle area calculations, computational details, and reference activity measurements. See DOI: 10.1039/x0xx00000x

COMMUNICATION

on compounds at the extremes of each compositional range or have used materials with poorly-defined morphologies, such as porous films or polydisperse nanoparticles.[18, 44, 45] In view of the extensive literature on transition metal chalcogenides[17, 21, 27, 46] and phosphides,[22, 23, 47] knowledge of the role of the anion in controlling these physicochemical properties can help to rationalize future design strategies for optimizing electrocatalytic activity.

In this work, we synthesize partially anion-exchanged nanoparticles (NPs) to determine how the anion substitution can affect electrocatalytic activity, using cobalt oxysulfide, CoO_xS_y, as a model system (**Fig. 1a**). We focus on the hydrogen evolution reaction electrocatalysis (HER, $2H_2O + 2e^- \leftrightarrow H_2 + 2OH^-$ in alkaline), which has been reported to be active on cobalt sulfides[43, 48-50] and other cobalt chalcogenides.[51] We show that the HER activity depends sensitively on the anion chemistry, which can subsequently be optimized during catalyst synthesis. Specifically, we demonstrate that there is an optimum composition for the HER electrocatalysis at relatively small levels of sulfide doping (**Fig. 1b**). We attribute the increased HER activity after anion exchange to the stronger hydrogen adsorption energy following the substitution of S^{2-} in place of O^{2-} in Co-oxysulfide, effectively reducing the intermediate energy during the HER.

To carry out the partial substitution of the anions, we use a protocol based on organic-phase colloidal synthesis. Colloidal NP synthesis offers many advantages, such as controlled nucleation and growth in solution, thereby producing particles with well-defined, highly-uniform size and shape.[52-55] The monodispersity that is afforded by colloidal synthesis offers an unprecedented opportunity to establish and optimize structure-activity relationships.[56, 57] Furthermore, the nanoscale nature of the produced materials can allow for non-conventional transformation kinetics, resulting in a metastable structure that is considered unobtainable according to the phase diagram.[58] A disadvantage of colloidal synthesis is the requirement of a surfactant to act as a stabilizer and particle growth regulator.[59-61] This requires a surface ligand removal step such as high-temperature annealing,[57] replacement of long-chain ligands with more volatile or soluble ones,[62, 63] or, as used in this work, ligand displacement using highly reactive inorganic species.[61, 64, 65]

Our method to create the anion-substituted series is based on our previous finding that ammonium sulfide, $(NH_4)_2S$, can insert S into oxides under relatively mild conditions.[66] In this work, we achieve partial substitution by limiting the amount of added $(NH_4)_2S$ to control the diffusion of an isovalent anionic dopant, S^{2-}, into organosoluble CoO_x NPs, thereby producing S-substituted $CoO_{x-y}S_y$ NPs (see schematic of this evolution **Fig. 2a**). Briefly, we first oxidize cobalt NPs into CoO_x[67] and then sulfidize them into CoO_xS_y NPs. The oxygen in the CoO_x is anion-exchanged for sulfur through the addition of $(NH_4)_2S$ dissolved in oleylamine to the CoO_x NP solution at 100°C under N_2 atmosphere. We explore the nominal molar ratios of $(NH_4)_2S$ to Co at 3:10 (dilute doping), 1:1, and 3:1 (excess sulfur). We also investigate the effect of annealing by re-suspending the NPs following re-isolation in an organic solvent followed by a 200°C heat-treatment under N_2 for 1 hour. These annealed NPs serve as a control to explore the phase stability of Co-oxysulfides following the anion substitution.

To assess the stoichiometry of the Co-oxysulfide particles, we apply inductively coupled plasma-optical emission spectrometry (ICP-OES). We find the approximate stoichiometries for the (non-annealed) doped samples to be $CoO_xS_{0.18}$, $CoO_xS_{1.03}$, and $CoO_xS_{1.27}$ for the $(NH_4)_2S$:Co molar ratios of 3:10, 1:1, and 3:1, respectively. Annealing the sample did not significantly alter its stoichiometry (see Supporting Information). This elemental analysis confirms that significant amounts of S, in direct proportion to the amount of $(NH_4)_2S$ used, are incorporated into the NPs. As observed previously,[66] under our conditions the resulting S:Co ratio in the NPs will not exceed the stoichiometry of Co_3S_4, even with a large excess of $(NH_4)_2S$.

The CoO_x NPs obtained after oxidation are hollow and polycrystalline, with a diameter of 13.0±1.5 nm (**Fig. 2b**). The most dilutely doped oxysulfide NPs ($CoO_xS_{0.18}$), created from the $(NH_4)_2S$:Co ratio of 3:10, retain a morphology virtually identical to the initial pure oxide NPs (diameter 12.9±1.4 nm) (**Fig. 2c**). Annealing the most dilutely doped NPs does not change the morphology (**Fig. S1**). For higher degrees of anion-exchange doping, the diameter increases ($CoO_xS_{1.03}$, 15.0±1.7 nm, **Fig. 2d**; $CoO_xS_{1.27}$, 14.5±1.6 nm, **Fig. 2e**). This increase is consistent with the previous report for cobalt oxide NPs fully anion-exchanged into cobalt sulfide NPs.[66] The increase in the particle size follows the growth of the cavity within the NPs as a result of the nanoscale Kirkendall effect.[67-69]

The structural changes in the sulfidized CoO_xS_y NPs are assessed using selected area electron diffraction (SAED) (**Fig. 2f**, and **Fig. S1**), showing that the CoO_x and $CoO_xS_{0.18}$ NPs exhibit a rock-salt structure with broad reflections from the (111), (200), and (220) planes. Close examination of the rotationally averaged SAED patterns shows that the crystal structures for these NPs agrees well with the reference CoO structure; however, the $CoO_xS_{0.18}$ SAED pattern exhibits a small shift to lower scattering angles, indicating an expansion of the unit cell (vertical dashed line in **Fig. 2f**). Lattice expansion could be caused by the larger S anion occupying the O^{2-} lattice. Based on the magnitude of the shift, however, the calculated increase in unit cell size is, at most, 0.02 Å relative to the reference structure for CoO. Interestingly, this shift is an order of magnitude less than what one might expect based on the extrapolation of the Co-O/Co-S bond lengths from the Shannon radii[70] (see Supporting Information). We therefore anticipate that the S concentration at the surface may be higher than in the bulk.

To develop an intuition for this shift, we include the SAED pattern for an annealed Co oxysulfide sample that was prepared in the same way as $CoO_xS_{0.18}$ (using a 3:10 $(NH_4)_2S$:Co molar ratio, **Fig. 2f**, blue dashed line). ICP-OES for this sample revealed a composition of $CoO_xS_{0.17}$, similar to that of the unannealed NPs. As shown in **Fig. 2f**, the lattice spacing for the heat-treated $CoO_xS_{0.17}$ sample is more similar to the CoO reference than the unannealed $CoO_xS_{0.18}$ NPs. We interpret this finding as an indication of phase separation in the annealed samples ($CoO_xS_{0.17}$) into CoO and either the Co_9S_8 or the Co_3S_4
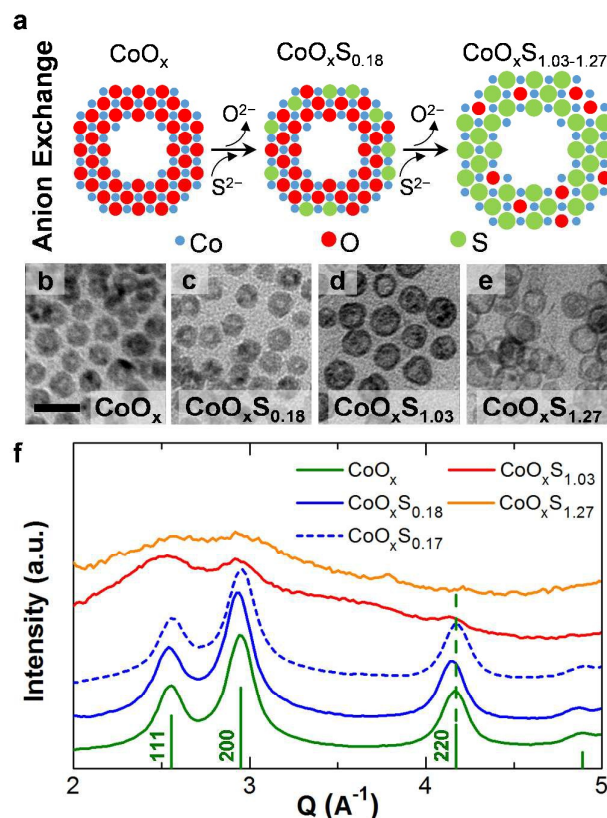
Figure 2. Schematic of the synthesis of cobalt oxysulfides via partial and "full" anion exchange (**a**). Transmission electron microscopy characterization of structural transformations of CoO_xS_y nanoparticles during anion exchange (**a**) of O^{2-} with S^{2-} (**b-e**, scale bar 25 nm) and the rotationally averaged SAED patterns (**f**). The particle morphology and crystal structure of the CoO_x particles (**b**) are retained at low S^{2-} doping levels (**c**), but at higher doping levels the particles swell and become less crystalline (**d,e**). Reference lines are given in (**f**) for CoO (JCPDS 00-048-1719); the dashed vertical line identifies the (220) reflection, at which the shifts are most apparent.

phase. In contrast, we believe the data indicates the unannealed $CoO_xS_{0.18}$ sample has sulfur occupying the anion sites in the rock salt structure. We did not, however, observe reflections for the Co_9S_8 or Co_3S_4 phases. We hypothesize that these sulfides must have domain sizes too small to give observable reflections or that they form amorphous phases during the phase separation process (see Supporting Information). As we will show later in our first-principles calculations, the two-phase nature is the energetically favourable phase in the Co oxysulfide material.

We further increase sulfur substitution by using higher $(NH_4)_2S$:Co ratios (1:1 and 1:3) to increase the driving force for S incorporation. At these high S concentrations, the particles ($CoO_xS_{1.03}$ and $CoO_xS_{1.27}$) become partially crystalline or amorphous (**Fig. 2 d,e**). We observe weak peaks that could correspond to smaller grains of CoO in the $CoO_xS_{1.03}$ samples (approximately 15 Å in size, compared to about 30 Å for CoO_x and dilutely doped samples as estimated by the Scherrer equation; see **Table S1**). With more sulfur addition, the primary rocksalt CoO reflections become very weak in $CoO_xS_{1.27}$. Annealing the-

se Co oxysulfide NPs leads to a significant solid-state reconstruction within the NPs, which results in a phase separation into a structurally distorted oxide and sulfide (see Supporting Information). We note that this phase separation occurs without significantly changing the compositions. The annealed Co oxysulfides have stoichiometries of $CoO_xS_{0.88}$ and $CoO_xS_{1.26}$ for the $(NH_4)_2S$:Co molar ratios 1:1 and 1:3, respectively, similar to those of the unannealed Co oxysulfides ($CoO_xS_{1.03}$ and $CoO_xS_{1.27}$). These annealed, higher sulfur-content NPs show a much less pronounced expansion in size relative to the starting NPs compared to their non-annealed analogues (see **Fig. S1a-h**).

To better understand the substitution mechanism of S^{2-} for O^{2-}, we perform density-functional theory (DFT) calculations to study the energetics of the Co oxysulfide system (see Supporting Information). We find that although it is thermodynamically favorable for S^{2-} to reside in place of O^{2-}, the migration energy barrier for S^{2-} diffusion through CoO is significant (2.63 eV, as compared to 0.18 eV for Co), preventing rapid movement into the CoO_x NPs.[66] These observations support the possibility that S^{2-} substitutes in place of O^{2-} through under-coordinated surface and defect sites, as has been observed for sulfidized MoP.[40] Our calculations of the formation energies of different phases in the Co-O-S system suggest that mixtures of CoO and Co-sulfide phases (Co_9S_8 and Co_3S_4) are significantly lower in energy than the rocksalt CoO_xS_y structures. This DFT finding is consistent with the observed phase separation seen by SAED. We therefore propose that the unannealed Co oxysulfides are a metastable phase characterized by the substitution of sulfur onto the under-coordinated anion sites. With more introduced sulfide, the driving force for sulfidization becomes large enough that Co rapidly diffuses outward,[66] forming an amorphous phase. Upon annealing, phase separation occurs, allowing the NPs to form Co-sulfide domains (Co_9S_8 and Co_3S_4). At the lowest $(NH_4)_2S$:Co ratio, the resulting grains of Co-sulfide are likely too small to be observed.

To understand how the anionic substitution affects the electrochemical properties, we conducted cyclic voltammetry (CV) experiments in Ar-saturated 0.1M KOH. **Fig. 3** shows the CV results of the NPs examined using a thin-film electrode prepared from a composite of the NPs, acetylene black, and K^+-Nafion®.[71] To ensure that the electrochemical response of these NPs is intrinsic to the surface chemistry, we treated the NPs with 0.1 M KOH in isopropanol under sonication for 30 minutes to strip off the ligands.[64, 65] To ensure ligand removal, we compared the CV result of our CoO_x NPs to thin-film electrodes prepared in the same manner using nanopowders of known stoichiometry (CoO and Co_3O_4). The CoO reference showed a similar electrochemical response to our CoO_x NPs (see **Fig. S2**), confirming the surface chemistry of our CoO_x NPs. We point out that the CV of our CoO_x NPs is distinct from that of the Co_3O_4 reference, supporting our conclusion that the CoO_x catalyst has a surface CoO crystal structure.

Our CV results capture the evolution of the surface chemistry of the Co oxysulfide particles throughout the anion substitution process. Notably, although CoO_x and $CoO_xS_{0.18}$ share the same crystal structure (**Fig. 2f**), their surface chemistries as
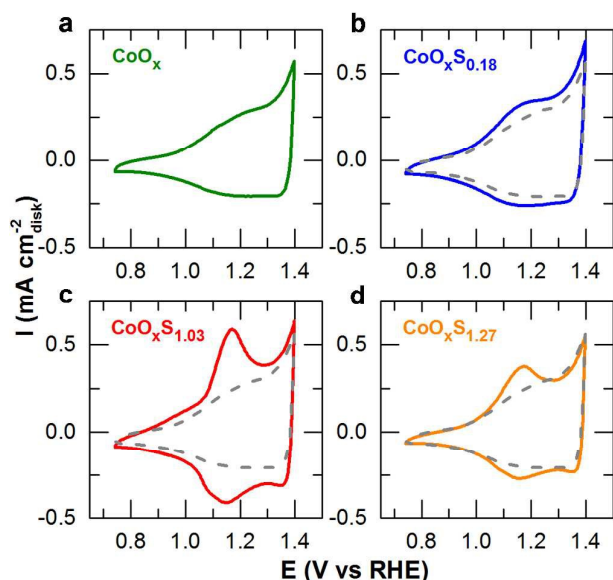
Figure 3. Cyclic voltammograms of carbon-supported thin-film electrocatalysts containing (samples not subjected to annealing) CoO_x (**a**), $CoO_xS_{0.18}$ (**b**), $CoO_xS_{1.03}$ (**c**), and $CoO_xS_{1.27}$ (**d**) nanoparticle electrocatalysts in Ar-saturated 0.1 M KOH at 50 mV/s scan rate. The grey dashed background CV in (**b**)-(**d**) shows a comparison to the CoO_x starting material.

revealed by the CV measurement are distinct. The starting CoO_x material shows a broad, shallow redox peak between ~1.0 and ~1.3 V vs. RHE, which is consistent with the Co^{2+}/Co^{3+} redox couple in literature (**Fig. 3a**).[31, 72, 73] With the inclusion of more S^{2-}, a reversible peak in the region of 1.1 V vs. RHE grows (**Fig. 3b-d**). This observation is consistent with previous reports on Co sulfides, which have suggested that this redox couple can be attributed to the reaction(s) $CoS + OH^- \leftrightarrow CoS-OH + H_2O + e^-$ and/or $CoS-OH + OH^- \leftrightarrow CoSO + H_2O + e^-$.[74, 75] This assignment is consistent with the growth of the ~1.1 V vs. RHE peak $CoO_xS_{1.03}$ sample with the addition of S^{2-}, but we caution that future work remains to be done to verify the nature of this redox couple. Interestingly, the peak height decreases for the $CoO_xS_{1.27}$ sample. At the moment, it is unclear what causes the peak height to decrease.

We characterize the HER activity on these partially-anion-substituted materials in an H_2-saturated 0.1 M KOH electrolyte at 10 mV/s (**Fig. 4a**). The polarization curves show that the addition of sulfur improves the HER activity beyond that of CoO_x. The improvement in the HER activity is most pronounced for the most dilute doping ($CoO_xS_{0.18}$). In comparison to the starting CoO_x material: the specific HER activity of $CoO_xS_{0.18}$ is ~3x more than the CoO_x starting material at -375 mV (vs. RHE). Further addition of S^{2-} does not sustain this increase in activity; the observed HER activity returns to a level close to that of CoO_x for samples with additional S^{2-} beyond $CoO_xS_{0.18}$. These results are summarized in the corresponding Tafel plots (**Fig. 4b** and **Fig. S3**). Interestingly, the CoO_x, $CoO_xS_{1.03}$, and $CoO_xS_{1.27}$ samples exhibit a large Tafel slope of 160-170 mV/decade, which corresponds to the phenomenological transfer coefficient (α) of ~1/3, while the $CoO_xS_{0.18}$ sample shows a Tafel slope of 200 mV/decade. These transfer

coefficients are significantly larger than the reported Tafel slopes for metals[76, 77] and other sulfide catalysts.[16, 17, 51] Future work in understanding this rather high Tafel slope is essential to pinpoint the microscopic mechanism for the observed enhancement in the HER.

To understand the origin of the HER activity enhancement, which was experimentally observed to be most effective at low S concentration, we apply the activity descriptor approach pioneered by Parsons, Gerischer, and Norskov.[26, 78] In this approach, the H adsorption energy estimates the surface's ability to form the HER intermediate.[79] We calculate the H adsorption energy on the CoO(100) surface, which is charge neutral and lowest in energy, as a function of the surface S composition using DFT (see Supporting Information, **Fig. S4**). In this framework, the most active HER electrocatalyst should have the H adsorption energy at a value that minimizes the energy difference between the reactant, the intermediate (H*), and the product. Generally, this value is found to be around the H adsorption energy on Pt.[26, 79, 80]

We observe that H* prefers to bind to a Co ion rather than an O or S ion. Further analysis shows that H* develops a partial negative charge, explaining its tendency to sit above a positively charged Co ion. As we substitute more S onto the surface, the H* absorption energy first decreases, indicating stronger bonding between H* and Co. Crucially, at an average of only 1 in 8 O^{2-} ions substituted with S^{2-} on a CoO(100) surface 2×2 unit cell, the adsorption energy of H approaches that of Pt(111), which we use as a benchmark for an "ideal" HER catalyst (**Fig. 5**, blue plot). Also plotted are the experimentally determined values for HER current at 375 mV, as a function of S:Co ratio (**Fig. 5**, red plot). As more O is displaced, the H binding energy returns to the initially high value. Assuming that the thermodynamic formation of the adsorbed H intermediate limits the HER kinetics,[27, 79-81] our DFT calculations broadly agree with our experimental HER results. Specifically, the reduction in the H adsorption energy following the partial S^{2-} exchange increases HER activity initially; however, as more
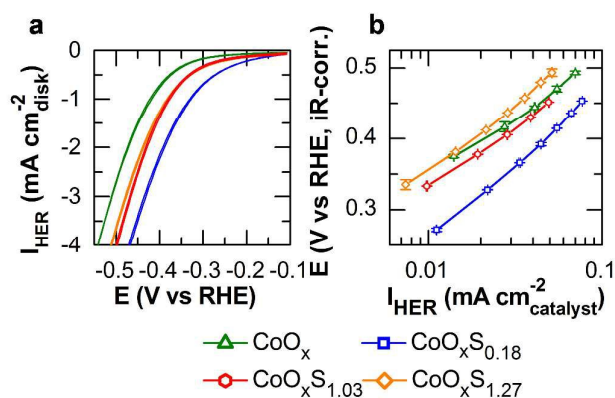

Figure 4. Polarization curves of carbon-supported thin-film electrocatalysts containing cobalt oxide/oxysulfides (samples not subjected to annealing). Geometric hydrogen evolution current densities (**a**) were measured in H_2-saturated 0.1M KOH at 10 mV/s. A Tafel plot (**b**) is shown based on the known geometries of the particles. Error bars in (**b**) give the standard deviation from three independent measurements.
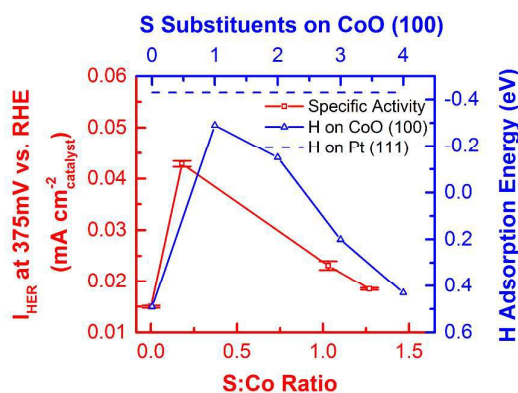
Figure 5. Calculated DFT adsorption energies of hydrogen and their correlation with experimental results for the activity of CoO_xS_y nanoparticle electrocatalysts (error bars give the standard deviation based on three independent measurements). At low doping levels (e.g., $CoO_xS_{0.18}$) the experimentally-determined HER specific activity of the particles substantially increases (red curve) while at higher doping levels, activity decreases. This activity change is a result of S^{2-} strengthening the H adsorption energy on the CoO surface (blue curve), bringing it closer to the H adsorption energy on Pt(111) (blue dashed curve) at low S^{2-} doping levels.

sulfur is incorporated, the formation of the H* intermediate becomes more energetically intensive and consequently impedes the HER kinetics. We emphasize not just that isovalent anionic dopants may be used to tune the hydrogen adsorption free energy to optimize electrocatalytic activity but also that the composition of the doped electrocatalyst must be precisely tuned in order to exploit the surface's ability to facilitate an electrochemical reaction. To emphasize the importance of the anion control, we show through our HER measurement on sulfur-rich CoS_2 nanoparticles that the HER electrocatalysis on CoS_2 is also not as high our Co-oxysulfide nanoparticles (see **Fig. S7-S8**). Recent results from others also reach a similar conclusion as ours, highlighting the need for an anion control .[41, 42]

In summary, we report the critical role of an isovalent anionic substitution in controlling the electrocatalytic activity of a transition-metal-containing electrocatalyst. As shown in the Co oxysulfide system, anionic substitution can positively affect the HER activity; however, the substitution process must be tightly controlled to obtain the desired enhancement. In our cobalt oxysulfide nanoparticles, we accomplish this control by engineering the anion-exchange driving force by adjusting the amount of the highly reactive S^{2-} precursor. Using this protocol, we produce a series of cobalt oxysulfide nanoparticles with different amounts of S^{2-}, which allow us to establish the trend between the HER activity and the sulfide content. We find a small amount of S is best for enhancing the HER; further sulfur addition disrupts the H* intermediate energy and also alters the phase of the oxysulfides. We attribute the activity enhancement at low S^{2-} concentration to a 'dopant' effect, whereby the presence of the S^{2-} in the surface layer modifies the hydrogen adsorption on the oxysulfide electrocatalyst. Our results highlight an opportunity to control the anionic composition as a strategy for not just clarifying the role of the anions but also for further increasing the activity of electrocatalysts.

References

1. J. Greeley and N. M. Markovic, *Energy and Environmental Science*, 2012, **5**, 9246-9256.
2. J. Greeley, I. E. L. Stephens, A. S. Bondarenko, T. P. Johansson, H. A. Hansen, T. F. Jaramillo, J. Rossmeisl, I. Chorkendorff and J. K. Nørskov, *Nature Chemistry*, 2009, **1**, 552-556.
3. I. E. L. Stephens, A. S. Bondarenko, U. Grønbjerg, J. Rossmeisl and I. Chorkendorff, *Energy and Environmental Science*, 2012, **5**, 6744-6762.
4. W. Sheng, A. P. Bivens, M. Myint, Z. Zhuang, R. V. Forest, Q. Fang, J. G. Chen and Y. Yan, *Energy and Environmental Science*, 2014, **7**, 1719-1724.
5. D. V. Esposito, S. T. Hunt, Y. C. Kimmel and J. G. Chen, *Journal of the American Chemical Society*, 2012, **134**, 3025-3033.
6. Z. Han, F. Qiu, R. Eisenberg, P. L. Holland and T. D. Krauss, *Science*, 2012, **338**, 1321-1324
7. T. Y. Ma, J. Ran, S. Dai, M. Jaroniec and S. Z. Qiao, *Angewandte Chemie International Edition*, 2014, **54**, 4646–4650.
8. W. Zhou, Y. Zhou, L. Yang, J. Huang, Y. Ke, K. Zhou, L. Li and S. Chen, *Journal of Materials Chemistry A*, 2015, **3**, 1915-1919.
9. W. Zhou, J. Zhou, Y. Zhou, J. Lu, K. Zhou, L. Yang, Z. Tang, L. Li and S. Chen, *Chemistry of Materials*, 2015, **27**, 2026–2032.
10. T. Y. Ma, S. Dai, M. Jaroniec and S. Z. Qiao, *Journal of the American Chemical Society*, 2014, **136**, 13925–13931.
11. W. T. Hong, M. Risch, K. A. Stoerzinger, A. Grimaud, J. Suntivich and Y. Shao-Horn, *Energy and Environmental Science*, 2015, **8**, 1404-1427.
12. T. R. Cook, D. K. Dogutan, S. Y. Reece, Y. Surendranath, T. S. Teets and D. G. Nocera, *Chemical Reviews*, 2010, **110**, 6474-6502.
13. T. Maiyalagan, K. A. Jarvis, S. Therese, P. J. Ferreira and A. Manthiram, *Nature Communications*, 2014, **5**, 1-8.
14. D. M. Robinson, Y. B. Go, M. Mui, G. Gardner, Z. Zhang, D. Mastrogiovanni, E. Garfunkel, J. Li, M. Greenblatt and G. C. Dismukes, *Journal of the American Chemical Society*, 2013, **135**, 3494-3501.
15. H. Cheng, Y.-Z. Su, P.-Y. Kuang, G.-F. Chen and Z.-Q. Liu, *Journal of Materials Chemistry A*, 2015, **3**, 19314-19321.

16. J. M. Falkowski, N. M. Concannon, B. Yan and Y. Surendranath, *Journal of the American Chemical Society*, 2015, **137**, 7978–7981.

17. J. D. Benck, T. R. Hellstern, J. Kibsgaard, P. Chakthranont and T. F. Jaramillo, *ACS Catalysis*, 2014, **4**, 3957-3971.

18. X. Liu, J. Du, C. Li, X. Han, X. Hu, F. Cheng and J. Chen, *Journal of Materials Chemistry A*, 2015, **3**, 3425-3431.

19. Y.-F. Xu, M.-R. Gao, Y.-R. Zheng, J. Jiang and S.-H. Yu, *Angewandte Chemie International Edition*, 2013, **52**, 8546-8550.

20. J. Huang, D. Hou, Y. Zhou, W. Zhou, G. Li, Z. Tang, L. Li and S. Chen, *Journal of Materials Chemistry A*, 2015, **3**, 22886-22891.

21. W. Zhou, X.-J. Wu, X. Cao, X. Huang, C. Tan, J. Tian, H. Liu, J. Wang and H. Zhang, *Energy and Environmental Science*, 2013, **6**, 2921-2924.

22. J. Tian, Q. Liu, A. M. Asiri and X. Sun, *Journal of the American Chemical Society*, 2014, **136**, 7587-7590.

23. E. J. Popczun, J. R. McKone, C. G. Read, A. J. Biacchi, A. M. Wiltrout, N. S. Lewis and R. E. Schaak, *Journal of the American Chemical Society*, 2013, **135**, 9267-9270.

24. L. Feng, H. Vrubel, M. Bensimon and X. Hu, *Physical Chemistry Chemical Physics*, 2014, **16**, 5917-5921.

25. J. Suntivich, K. J. May, H. A. Gasteiger, J. B. Goodenough and Y. Shao-Horn, *Science*, 2011, **334**, 1383-1385

26. J. K. Nørskov, T. Bligaard, A. Logadottir, J. R. Kitchin, J. G. Chen, S. Pandelov and U. Stimming, *Journal of the Electrochemical Society*, 2005, **152**, J23-J26.

27. T. F. Jaramillo, K. P. Jorgensen, J. Bonde, J. H. Nielsen, S. Horch and I. Chorkendorff, *Science* 2007, **317**, 100-102.

28. J. Bonde, P. G. Moses, T. F. Jaramillo, J. K. Nørskov and I. Chorkendorff, *Faraday Discussions*, 2009, **140**, 219-231.

29. A. Grimaud, K. J. May, C. E. Carlton, Y.-L. Lee, M. Risch, W. T. Hong, J. Zhou and Y. Shao-Horn, *Nature Communications*, 2013, **4**.

30. F. Calle-Vallejo, N. G. Inoglu, H.-Y. Su, J. I. Martínez, I. C. Man, M. T. M. Koper, J. R. Kitchin and J. Rossmeisl, *Chemical Science*, 2013, **4**, 1245-1249.

31. L. Trotochaud, J. K. Ranney, K. N. Williams and S. W. Boettcher, *Journal of the American Chemical Society*, 2012, **134**, 17253–17261.

32. H. Zhu, S. Zhang, Y.-X. Huang, L. Wu and S. Sun, *Nano Letters*, 2013, **13**, 2947-2951.

33. E. Schmidt, *Solid State Ionics* 1995, **76**, 243-247.

34. K. Ueda, H. Hiramatsu, M. Hirano, T. Kamiya and H. Hosono, *Thin Solid Films* 2006, **496**, 8-15.

35. R. Asahi, T. Morikawa, T. Ohwaki, K. Aoki and Y. Taga, *Science* 2001, **293**, 269-271.

36. W. J. Zhou, Y. H. Leng, D. M. Hou, H. D. Li, L. G. Li, G. Q. Li, H. Liu and S. W. Chen, *Nanoscale*, 2014, **6**, 4698-4704.

37. Q. Gong, L. Cheng, C. Liu, M. Zhang, Q. Feng, H. Ye, M. Zeng, L. Xie, Z. Liu and Y. Li, *ACS Catalysis*, 2015, **5**, 2213–2219.

38. Z. Xu, H. Wang, Z. Li, A. Kohandehghan, J. Ding, J. Chen, K. Cui and D. Mitlin, *The Journal of Physical Chemistry C*, 2014, **118**, 18387-18396.

39. Z. Chen, D. Cummins, B. N. Reinecke, E. Clark, M. K. Sunkara and T. F. Jaramillo, *Nano Letters*, 2011, **11**, 4168–4175.

40. J. Kibsgaard and T. F. Jaramillo, *Angewandte Chemie International Edition*, 2014, **53**, 14433-14437.

41. M. L. S. Miguel Cabán-Acevedo, J. R. Schmidt, Joseph G. Thomas, Qi Ding, Hung-Chih Chang, Meng-Lin Tsai, Jr-Hau He, Song Jin, *Nature Materials*, 2015.

42. J. Zhuo, Miguel Caban-Acevedo, H. Liang, L. Samad, Q. Ding, Y. Fu, M. Li and a. S. Jin, *ACS Catalysis*, 2015, **5**, 6355-6361.

43. Y. Sun, C. Liu, D. C. Grauer, J. Yano, J. R. Long, P. Yang and C. J. Chang, *Journal of the American Chemical Society* 2013, **135**, 17699-17702.

44. I. T. Sines, D. D. Vaughn, A. J. Biacchi, C. E. Kingsley, E. J. Popczun and R. E. Schaak, *Chemistry of Materials*, 2012, **24**, 3088–3093.

45. Y. Xu, R. Wu, J. Zhang, Y. Shia and B. Zhang, *Chemical Communications*, 2013, **49**, 6656-6658.

46. D. Kong, J. J. Cha, H. Wang, H. R. Lee and Y. Cui, *Energy and Environmental Science*, 2013, **6**, 3553-3558.

47. J. F. Callejas, C. G. Read, E. J. Popczun, J. M. McEnaney and R. E. Schaak, *Chemistry of Materials*, 2015, **27**, 3769-3774.

48. M. S. Faber, M. A. Lukowski, Q. Ding, N. S. Kaiser and S. Jin, *The Journal of Physical Chemistry C* 2014, **118**, 21347-21356.

49. H. Zhang, Y. Li, G. Zhang, T. Xu, P. Wan and X. Sun, *Journal of Materials Chemistry A*, 2015, **3**, 6306-6310.

50. L.-L. Feng, G.-D. Li, Y. Liu, Y. Wu, H. Chen, Y. Wang, Y.-C. Zou, D. Wang and X. Zou, *ACS Applied Materials & Interfaces* 2015, **7**, 980-988.

51. D. Kong, H. Wang, Z. Lu and Y. Cui, *Journal of the American Chemical Society*, 2014, **136**, 4897-4900.

52. Y. Yin and A. P. Alivisatos, *Nature*, 2004, **437**, 664-670.

53. V. F. Puntes, K. M. Krishnan and A. P. Alivisatos, *Science*, 2001, **291**, 2115-2117.

54. Z. Peng and H. Yang, *Nano Today*, 2009, **4**, 143-164.

55. D. J. Milliron, S. M. Hughes, Y. Cui, L. Manna, J. Li, L.-W. Wang and A. P. Alivisatos, *Nature*, 2004, **430**, 190-195.

56. S. Zhang, X. Zhang, G. Jiang, H. Zhu, S. Guo, D. Su, G. Lu and S. Sun, *Journal of the American Chemical Society*, 2014, **136**, 7734-7739.

57. M. Cargnello, C. Chen, B. T. Diroll, V. V. T. Doan-Nguyen, R. J. Gorte and C. B. Murray, *Journal of the American Chemical Society*, 2015, **137**, 6906-6911.

58. M. Fayette and R. D. Robinson, *Journal of Materials Chemistry A*, 2014, **2**, 5965-5978.

59. Z. Niu and Y. Li, *Chemistry of Materials*, 2014, **26**, 72-83.

60. D. Li, C. Wang, D. Tripkovic, S. Sun, N. M. Markovic and V. R. Stamenkovic, *ACS Catalysis*, 2012, **2**, 1358-1362.

61. E. L. Rosen, R. Buonsanti, A. Llordes, A. M. Sawvel, D. J. Milliron and B. A. Helms, *Angewandte Chemie International Edition*, 2012, **51**, 684-689.

62. H. You, W. Wang and S. Yang, *ACS Applied Materials and Interfaces*, 2014, **6**, 19035–19040.

63. J. Wu, J. Zhang, Z. Peng, S. Yang, F. T. Wagner and H. Yang, *Journal of the American Chemical Society*, 2010, **132**, 4984-4985.

64. H. Zhang, B. Hu, L. Sun, R. Hovden, F. W. Wise, D. A. Muller and R. D. Robinson, *Nano Letters*, 2011, **11**, 5356-5361.

65. D. Weber, R. Sharma, S. Botnaras, D. V. Pham, J. Steiger and L. D. Cola, *Journal of Materials Chemistry C*, 2013, **1**, 7111-7116.

66. H. Zhang, L. V. Solomon, D.-H. Ha, S. Honrao, R. G. Hennig and R. D. Robinson, *Dalton Transactions*, 2013, **42**, 12596-12599.
67. Y. Yin, R. M. Rioux, C. K. Erdonmez, S. Hughes, G. A. Somorjai and A. P. Alivisatos, *Science*, 2004, **304**, 711-714.
68. J. Park, H. Zheng, Y.-w. Jun and A. P. Alivisatos, *Journal of the American Chemical Society*, 2009, **131**, 13943–13945.
69. A. Cabot, V. F. Puntes, E. Shevchenko, Y. Yin, L. Balcells, M. A. Marcus, S. M. Hughes and A. P. Alivisatos, *2007*, 2007, **129**, 10358–10360.
70. R. D. Shannon, *Acta Crystallographica*, 1976, **A32**, 751-767.
71. J. Suntivich, H. A. Gasteiger, N. Yabuuchi and Y. Shao-Horn, *Journal of the Electrochemical Society*, 2010, **157**, 81263-81268.
72. I. G. Casella, *Journal of Electroanalytical Chemistry*, 2002, **520**, 119-125.
73. I. G. Casella and M. R. Guascito, *Electrochimica Acta*, 1999, **45**, 1113-1120.
74. Q. Wang, L. Jiao, H. Du, Y. Si, Y. Wang and H. Yuan, *Journal of Materials Chemistry*, 2012, **22**, 21387.
75. F. Tao, Y.-Q. Zhao, G.-Q. Zhang and H.-L. Li, *Electrochemistry Communications*, 2007, **9**, 1282-1287.
76. J. O. M. Bockris, I. A. Ammar and A. K. M. S. Hug, *Journal of Physical Chemistry*, 1957, **61**, 879-886.
77. B. E. Conway and B. V. Titak, *Electrochimica Acta*, 2002, **47**, 3571-3594.
78. R. Parsons, *Transactions of the Faraday Society*, 1958, **54**, 1053-1063.
79. J. Greeley, J. Nørskov, L. A. Kibler, A. M. El-Aziz and D. M. Kolb, *ChemPhysChem*, 2006, **7**, 1032-1035.
80. W. Sheng, M. Myint, J. G. Chen and Y. Yan, *Energy and Environmental Science*, 2013, **6**, 1509-1512.
81. J. Greeley, T. F. Jaramillo, J. Bonde, I. Chorkendorff and J. K. Nørskov, *Nature Materials*, 2006, **5**, 909-913.